Acta Geotechnica
https://doi.org/10.1007/s11440-022-01715-1

RESEARCH PAPER

Numerical investigations of enhanced shallow geothermal energy recovery using microencapsulated phase change materials and metal fins

Yimin Lu[1] · Douglas D. Cortes[2] · Xiong (Bill) Yu[3] · Guillermo Narsilio[4] · Sheng Dai[1]

Received: 15 October 2021 / Accepted: 23 September 2022

Abstract
The efficiency of shallow geothermal energy recovery has been constrained by both the short-term temperature anomaly around heat exchangers and the long-term ground heat depletion. This study presents numerical investigations of significant improvement in the thermal performance of energy piles by using microencapsulated phase change materials (mPCM) and metal fins in the ground. A three-dimensional hydrothermal FEM model of an energy pile embedded in the ground is developed, validated, and extended to consider phase change and latent heat in the ground to evaluate the thermal performance of the energy pile under various ground conditions. The results show that both the energy harvest amount and efficiency can be evidently improved by mixing small proportions of mPCM in the ground to utilize its latent heat. The recovery energy from the sand–mPCM mixture is twice that of just sand and thrice that of the pure granular mPCM ground during seasonal operations. Moreover, the temperature influence zone is significantly shrinked in the sand–mPCM mixture ground. In addition, installing metal fins around the energy pile can accelerate heat conduction with the far field and furtherly improve the heat recovery efficiency. This study sheds light on efficient and environmentally friendly geothermal energy recovery using phase change materials.

Keywords Coupled modeling · Energy pile · Ground modification · Latent heat · Thermal efficiency

1 Introduction

Shallow geothermal energy, which is considered as a promising alternative for space heating and cooling, brings both economic benefits for stakeholders and environmental relief [31, 44, 50, 51, 62]. As envisioned by the US Department of Energy, geothermal energy can potentially reduce 356.3 million metric tons of CO_2 emissions and around 50 billion dollars of energy cost each year [36]. However, this potential has been impeded by the high installation cost, stakeholders' awareness, and marketing [3, 53]. Currently, geothermal energy only accounts for less than 1% of US energy consumption [27].

Shallow geothermal energy recovery usually uses a closed-loop system embedded in soils to form ground heat exchangers that extract (or inject) thermal energy from (or to) the ground. The high initial cost including drilling and installation of ground heat exchangers impacts the economic feasibility of utilizing shallow geothermal energy. To mitigate this issue, ground heat exchangers are combined with subsurface structures like piles, retaining walls, and tunnels to form energy infrastructures [2, 5–7, 14, 17, 24, 37, 39, 40]. Extensive studies have been conducted to understand their thermo-mechanical behavior [2, 5, 7], thermal performance [14, 24, 37, 40], the cost, and carbon abutment effectiveness [3, 4, 6, 24, 39].

✉ Sheng Dai
sheng.dai@ce.gatech.edu

1 School of Civil and Environmental Engineering, Georgia Institute of Technology, Atlanta, GA 30332, USA

2 Department of Civil Engineering, New Mexico State University, Las Cruces, NM 88003, USA

3 Department of Civil and Environmental Engineering, Case Western Reserve University, Cleveland, OH 44106, USA

4 Department of Infrastructure Engineering, The University of Melbourne, Parkville, VIC 3010, Australia

Published online: 03 December 2022

The short-term (hours to weeks typically) thermal performance of a ground heat exchanger is usually investigated through laboratory or field thermal response tests [29, 38, 47, 59]. The efficiency can be hindered by the temperature anomaly emerging around the heat exchanger, the extent of which is governed by the thermal demand, the heat exchanger's flow condition, and the thermophysical properties of the ground. The long-term (months to years) thermal radius of influence dictates the minimum spacing required between heat exchangers to avoid mutual thermal interferences or legal issues associated with the unintended depletion of neighboring thermal reservoirs [1, 10, 47, 48]. Complementarily, numerical investigations often serve as an approach to parametrically evaluate different influencing factors on the thermal performance of ground heat exchangers, such as geometry and configurations [20, 41, 42], material thermal properties [20, 32], circulating fluid velocity [20, 32], fluid loop configurations [8, 43, 47, 61], groundwater flow conditions [12, 13, 30], as well as long-term operations [45, 46]. In the long term (years), the unbalance between the sensible heat extracted from the ground during winter and that injected into the ground during summer, as well as the difference between the mean yearly temperature and the initial ground temperature, will result in progressive cooling or heating of the ground. Since optimal geothermal designs are predicated on the ground maintaining an average constant temperature and a narrow range between seasons, when ground temperature changes progressively, the efficiency of heat exchangers diminishes, even to the point of making it economically unviable to operate [9, 23, 25, 49].

Both the short-term and the long-term ground heat depletion can be mitigated by using phase change materials (PCMs) [16, 26, 33, 55]. Phase change materials release or absorb additional thermal energy (which is called latent heat) during phase change without an obvious temperature variation. Most phase transition involves solid and liquid states, and the energy will be released or absorbed by transiting from solid to liquid or vice versa, with a heat of fusion much higher than the sensible heat. For instance, ice requires 333.5 J/g to melt into water, while water needs only 4.18 J/g energy to rise one degree. This important feature makes PCMs favored in the energy storage industry [28, 52] and energy-efficient buildings [35, 57]. Commercial applications of PCMs typically use salt hydrates or petroleum derivatives like paraffin [57]. In shallow geothermal systems, PCMs can shift and redistribute in time the geothermal energy available in comparison with the typical consideration of conduction only (or conduction–convention) heat transfer mechanisms. PCMs can also be implemented within the ground components of the system like grout materials [16, 55] or mixed with concrete materials [26, 33] to enhance shallow geothermal energy recovery. Using PCMs to augment the ground thermal properties and ensued impacts to ground heat exchangers have not been previously investigated.

This study investigates the thermal performance of an energy pile embedded in soils mixed with microencapsulated phase change materials (mPCM). The microencapsulation of a PCM facilitates the preparation of PCM–soil mixtures to improve the ground thermal properties, and with the customized size of mPCM particles to fill the pore space of soil, minimal disturbance to soil mechanical performance is expected. A coupled hydrothermal finite element method (FEM) model is established and validated against a published field thermal response test. Then, the model is used to evaluate the thermal performance of the energy pile embedded in different surrounding materials of sands, mPCM, and sand–mPCM mixtures with and without water. Both short-term and 60-day operations of the system are studied to assess the merits of incorporating mPCM to mitigate progressive ground heat depletion. It is assumed that mPCM in the mixtures is not washed away due to rainfall or infiltration; this is reasonable given the relatively minor total head gradients induced and penetration depths. Groundwater flow is not considered in this work, but a subject of future work (see Sect. 3.7). Finally, we show that the thermal performance can be further improved by adding metal fins around the energy pile, considering that the heat conductivity of mPCMs is relatively low. The results shed light on improving the economic feasibility and long-term sustainability of enhanced shallow geothermal energy recovery and utilization.

2 Methods and materials

2.1 Theoretical framework

A three-dimensional hydrothermal finite element model is developed to simulate the heat transfer and thermal response of a concrete pile with diameter D_1 and depth H_1 in the ground (Fig. 1a). The pile is equipped with a U-shaped pipe to circulate fluid for ground heat exchange. In the pile and the ground, heat transfer is assumed to be dominated by heat conduction, while the fluid within the pipe is regarded as a line heat source. The governing equation in this process is the energy conservation for heat transfer in solids:

$$\rho_1 C_1^p \frac{\partial T_1}{\partial t} = \nabla \cdot (\lambda_1 \nabla T_1) - Q \tag{1}$$

where ρ_1, λ_1, C_1^p, and T_1 are the density, thermal conductivity, specific heat capacity, and temperature of concrete (pile) or ground; t represents the time; and Q is the heat source/sink representing the circulating fluid within the

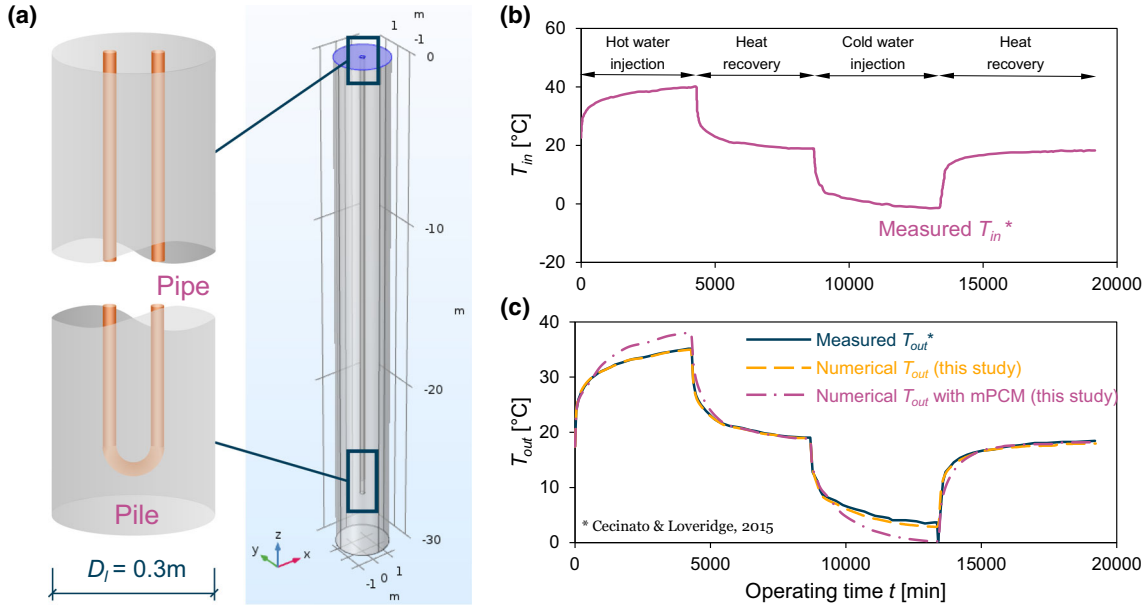

Fig. 1 Hydrothermal FEM model to simulate ground heat recovery. **a** An illustration of the model configuration. A concrete pile equipped with a U-shaped pipe is embedded in the ground with a constant initial temperature. Hot/cold fluid is circulated through the pipe to exchange heat with the ground. **b** Input temperature of the circulating fluid T_{in} measured in the field test [20]. **c** Output temperatures of the circulating fluid T_{out} from the field test [20] and numerical simulations of this study

pipe. Meanwhile, the heat transfer in the fluid is governed by both heat conduction and convection, and the surrounding solids are regarded as heat sources. The governing equations for this process are mass conservation, momentum conservation, and energy conservation:

$$\begin{cases} \dfrac{\partial \rho_2 A}{\partial t} + \nabla \cdot (\rho_2 A u) = 0 & (2a) \\ \rho_2 \dfrac{\partial A}{\partial t} + \rho_2 u \cdot \nabla u = -\nabla p - f_{\text{D}} \dfrac{\rho_2}{2 d_{\text{h}}} |u| u + F & (2b) \\ \rho_2 A C_2^p \dfrac{\partial T_2}{\partial t} + \rho_2 A C_2^p u \cdot \nabla T_2 = \nabla \cdot (\lambda_2 A \nabla T_2) + f_{\text{D}} \dfrac{\rho_2 A}{2 d_{\text{h}}} |u|^3 + Q + Q_{\text{p}} & (2c) \end{cases}$$

where ρ_2, λ_2, C_2^p, and T_2 are the density, thermal conductivity, specific heat capacity, and temperature of circulating fluid within the pipe; A and d_{h} represent the cross section area and the hydraulic diameter of the pipe; u and p stand for the fluid velocity and pressure; f_{D} is the Darcy friction factor; F represents the volume force; and Q_{p} and Q stand for the pipe and surrounding solids as heat source/sink. More detailed descriptions of the above-mentioned terms and coefficients can be referred to the COMSOL Multiphysics user's guide (COMSOL Multiphysics® v. 5.3a. www.comsol.com. COMSOL AB). Note also that the pipe flow is simulated as a one-dimensional flow, i.e., the representative temperature is the averaged temperature across the cross-sectional area of the pipe. The thermal and flow fields inside the pipe are considered fully developed, i.e., the entrance length is neglected.

The phase change phenomenon is modeled as happening smoothly within a small interval (i.e., 1 °C in this study) around the phase change temperature T_{phase} to avoid a sharp jump in the continuum simulation. A smooth function, $\theta(T)$, defined as the mass fraction of the phase before the transition and ranging from 0 to 1, is used to define the physical properties of the multiphase material. The thermal conductivity and the density of the PCM are expressed as

$$\lambda = \theta(T)\lambda_{\text{L}} + (1 - \theta(T))\lambda_{\text{S}} \quad (3)$$

$$\rho = \theta(T)\rho_{\text{L}} + (1 - \theta(T))\rho_{\text{S}} \quad (4)$$

where the subscripts L and S represent the liquid and the solid phases of PCMs. The specific heat capacity of the PCM is expressed as

$$C_{\text{p}} = \frac{1}{\rho}\left[\theta(T)\rho_{\text{L}} C_{\text{L}}^p + (1 - \theta(T))\rho_{\text{S}} C_{\text{S}}^p\right] + (\text{LH})\frac{\partial \alpha(T)}{\partial T} \quad (5)$$

where the last term regards the latent heat as an additional part of specific heat capacity using the apparent heat capacity method, in which (LH) is the latent heat and α is a smooth function preventing sharp jumps in continuum simulation:

$$\alpha(T) = \frac{1}{2}\frac{[1 - \theta(T)]\rho_{p2} - \theta(T)\rho_{p1}}{\rho}. \quad (6)$$

The above equations about phase change modeling contribute to Eq. (1) when simulating the ground medium with PCMs.

2.2 Model validation

The numerical model is implemented in the finite element package COMSOL and validated against a field thermal response test [20, 38]. This test reports the time-lapse input and output temperature of fluid circulated through a polyethylene pipe within a concrete pile with a 0.3 m diameter D_l and a 26.8 m length H_l. The pile is buried in a clayey medium with a constant initial temperature of 17.4 °C, a 3 m domain diameter D_s (i.e., 10 times the pile diameter D_l), and a 30 m depth H_s. The size of the ground domain is such that the heat transfer will not reach the boundary within the time period of the calibration test, so that no boundary effects come into the results. Thermal insulation, i.e., Neumann boundary condition of zero heat flux, is applied on the side and bottom boundaries of the ground domain. The Dirichlet boundary is applied to the ground surface, which is set at a constant temperature of 17.4 °C, identical to the initial temperature of the domain [38], and is assumed constant throughout the 14 days of the testing period. The air temperature fluctuations for this geometry should not influence the thermal response of this slender energy pile [15, 34]. Detailed dimensions, material parameters, and operating conditions [20, 38] are listed in Table 1. Note that the circulating fluid is often a mixture of water and antifreeze, and we use the built-in material model of water in COMSOL to represent the circulating fluid, whose physical and thermal properties are temperature-dependent (COMSOL Multiphysics® v. 5.3a. www.comsol.com. COMSOL AB 2017).

The field experiment [38] involves four stages: hot fluid injection, recovery, cold fluid injection, and recovery. The fluid temperature measured at the pipe inlet T_{in} during the four stages is shown in Fig. 1b. The numerically calculated fluid temperature at the pipe outlet using the field test geometry and properties (Table 1) agrees well with the field measurements, as shown in Fig. 1c.

Table 1 Parameters for model configuration and calibration [20, 38]

Type	Parameters	Values	Unit
Geometry	Inner diameter of pipe, d_p	0.0262	m
	Distance between two pipe legs, d_c	0.135	m
	Thickness of pipe wall, δ_p	0.0029	m
	Diameter of pile, D_l	0.3	m
	Depth of pile, H_l	26.8	m
	Diameter of ground/soil domain, D_s*	3	m
	Depth of ground/soil domain, H_s*	30	m
Pipe	Thermal conductivity of pipe, λ_p	0.385	W/m/K
Concrete pile	Density of concrete, ρ_l	2210	kg/m^3
	Specific heat capacity of concrete, C_l^p	1050	J/kg/K
	Thermal conductivity of concrete, λ_l	2.8	W/m/K
Soil	Density of soil, ρ_s	1900	kg/m^3
	Specific heat capacity of soil, C_s^p	1820	J/kg/K
	Thermal conductivity of soil, λ_s	2.3	W/m/K
Other	Mass flow rate at inlet, q_m	0.108	kg/s
	Initial temperature and surface temperature, T_i	17.4	°C

Subscripts: p = pipe, l = pile, s = soil. The diameter D_s and depth H_s of the ground domain used in the model calibration are assumed and not from the field test

2.3 Upgraded model considering phase change

To illustrate shallow geothermal energy recovery using phase change materials, the ground material is replaced by granular mPCM in the model. The mPCM particle consists of a large portion of paraffin in the core and a polymer encapsulation shell. The particle size of the mPCM used in this study is 15–30 μm with a tuned phase change temperature of 18 °C (Microtek LLC). This encapsulation makes paraffin a granular material compatible with soil and avoids soil contamination when melted. The density, thermal conductivity, latent heat, and specific heat capacity used in the simulation are ρ = 900 kg/m^3, λ = 0.23 W/m/K, LH = 185 kJ/kg, and C_p = 2981 J/kg/K (liquid) and 2604 J/kg/K (solid), respectively (see also Table 2 for details).

The output temperature obtained from the case of mPCM ground media is shown in Fig. 1c (dash-dotted line). Compared with the thermal response of the clayey ground, the mPCM case produces higher output temperature during hot fluid injection and lower output temperature during cold fluid injection, mainly due to the low thermal conductivity of the dry mPCM particles. This preliminary result contrasts the output thermal energy in ground media of clay versus mPCM particles, which implies inherently different heat transfer processes.

2.4 Material properties

Numerical simulations allow us to conduct parametric analyses of the impacts of thermal and physical properties of each component on the system thermal performance. The density and thermal properties of the materials used in this study are listed in Table 2. Three ground media are used in the simulations: sands, granular mPCM, and a sand–mPCM mixture, all assumed with a porosity of

Table 2 Material properties used in this simulation (l = liquid; s = solid)

Single-phase	Density ρ (kg/m^3)	Thermal conductivity λ (W/m/K)	Latent heat LH (kJ/kg)	Specific heat capacity C_p (J/kg/K)	Thermal diffusivity κ ($\times$ 10^{-7} m^2/s)
Quartz	2650	7.7 [18]	–	740 [56]	
Paraffin	900[b]	0.23 [54]	185[b]	2981 (l) [54]	
				2604 (s) [54]	
Water	1000	0.6 [18]	–	4192 (10 °C) [58]	
Air (20 °C)	0	0.03 [18]	–	–	
Mixture[a]	$\sum X_i f_i$	$\prod X_i^{f_i}$	$\frac{\sum X_i \rho_i f_i}{\sum \rho_i f_i}$	$\frac{\sum X_i \rho_i f_i}{\sum \rho_i f_i}$	$\kappa = \frac{\lambda}{\rho C_p}$
Sand					
Dry	1590	0.84	–	740	7.11
Saturated	1990	2.77	–	1434	9.72
mPCM					
Dry	540	0.10	185	2981 (l)	0.63 (l)
				2604 (s)	0.72 (s)
Saturated	940	0.34	106.3	3496 (l)	1.03 (l)
				3280 (s)	1.09 (s)
Sand-mPCM					
Dry	1806	1.36	22.13	1008 (l)	7.50 (l)
				963 (s)	7.85 (s)
Saturated	1966	2.20	20.33	1267 (l)	8.85 (l)
				1226 (s)	9.15 (s)

[a]X_i represents the corresponding property of each component, f_i stands for the volume fraction of each component. [b]Manufacturer data

n = 0.4. Note that the sand–mPCM mixture used here is considered as silty-sized mPCM particles (n = 0.4) filling the pores of sands (n = 0.4). That means the volume fraction of the mPCM is (1–0.4) × 0.4 = 0.24 in the mixture. All ground media are assumed either dry or fully water-saturated, and no unsaturated conditions are considered. The density and thermal properties of the three ground media are calculated using the properties of the single phase (i.e., quartz, paraffin, water, and air).

2.5 Thermal performance measurements

To quantify and contrast the thermal performance of different scenarios, we present the results in terms of the output thermal energy W_{out} [MJ], the output power P_{out} [kW], and a dimensionless power ratio R_{P} [−]. Specifically, the output thermal energy W_{out} measures the heat extracted from or injected into the ground and can be calculated by integrating the output power P_{out} with time t:

$$W_{\text{out}} = \int P_{\text{out}} \mathrm{d}t \tag{7}$$

where the output thermal power P_{out} is defined as

$$P_{\text{out}} = C^o_{p,w} \cdot q^o_v \cdot |T_{\text{out}} - T_{\text{in}}| \tag{8}$$

where $C^o_{\text{p,w}}$ stands for the specific heat capacity; T_{in} and T_{out} are the temperature at the inlet and outlet; and q^o_{v} is the volumetric flux at the loop outlet. Lastly, the power ratio R_{P}, a direct indicator of thermal energy recovery efficiency, is defined as

$$R_{\text{P}} = \frac{P_{\text{out}}}{P_{\text{in}}} \tag{9}$$

where P_{in} is the kinetic power consumed to circulate the fluid within the loop and equals the fluid pressure p_{in} times the volumetric flux q^i_{v} at the loop inlet:

$$P_{\text{in}} = p_{\text{in}} \cdot q^i_{\text{v}}. \tag{10}$$

2.6 Major assumptions in the simulations

According to the methodology described above, major assumptions used in this study include the following:

- Heat transfer in solids (i.e., the concrete pile and ground) is dominated by conduction, while the heat transfer in the fluid is governed by both conduction and

convection, and the fluid within the pipe is regarded as a line heat source.
- The pipe flow is modeled as one-dimensional neglecting radial and circumferential dimensions. The fluid temperature at any position along the pipe is the averaged temperature across the cross-sectional area at that position. The thermal and flow fields inside the pipe are considered fully developed, i.e., neglecting the entrance length.
- The ground surface is assumed at a constant temperature (Dirichlet boundary), and the other boundaries are considered to have no heat flux (Neumann boundary). The ground domain initially has a constant temperature.
- For phase change modeling, the latent heat is simulated as an additional part of the specific heat capacity of the PCM material.
- The porosity of ground media materials (sand, granular mPCM, and sand–mPCM mixture) is assumed as 0.4. The thermal conductivity of the mixture satisfies the geometric mean model. We acknowledge that packing has a significant role in the heat transfer processes in soils and the porosity used here reflects a cubic tetrahedral packing.

3 Analyses and discussion of results

In this section, we evaluate the effects of various material parameters and operational conditions on the thermal performance of an energy pile. The ground initial temperature is assumed to be 20 °C, and the injecting fluid temperature is 0 °C (e.g., a ground heat extraction scenario). Note that all the numerical parameters used in this section are the same as the validation model (Table 1, no phase change) if not been further specified in each subsection.

With the model setup (geometry, material, boundary, and operational conditions) of the thermal response test used in the model validation, we perform either 10-day continuous fluid injection standing for a typical short-term operation in practice, or 60-day on-and-off injection representing a typical longer-term operation in real life (Sect. 3.4). In each scenario, the thermal response reaches a quasi-steady state, which facilitates the quantitative comparison among different cases.

3.1 Effects of material thermal properties

Material thermal properties are basic but the most important parameters to decode the heat transfer process during shallow geothermal energy recovery. This section evaluates how the thermal performance of an energy pile is influenced by the thermal properties of the ground and the pile.

Figure 2 shows the output power P_{out} and power ratio R_P after a 10-day fluid circulation with changing thermal conductivity λ, specific heat capacity C_p, and density ρ of the ground and the pile. Note that some values of these properties may not be physically possible and the results here are to amplify the impacts of a wide range of parametric property values on the thermal performance.

In general, the trends of P_{out} and R_P with changing thermal parameters are similar, mainly due to the nearly identical input power P_{in} that is governed by the pipe geometry (diameter, length) and fluid flow (velocity, flux). Although the properties of fluid used here are temperature dependent, the difference in the input power P_{in} to circulate the fluid caused by temperature is negligible. The results in Fig. 2 highlight and confirm that the thermal performance is the most sensitive to the thermal conductivity, compared to the specific heat capacity and the density of the materials, and also that increasing the density and thermal properties of the ground rather than that of the pile is more efficient in recovering the thermal energy. In the scenario of continuous heat recovery for 10 days, the temperature influence zone had expanded to a much larger domain (than the size of the pile) within the ground, and thus the recoverable thermal energy stored in the pile becomes negligible compared to that from the ground. Therefore, the density and the specific heat capacity of the pile, governing how much energy can be extracted from the pile, have marginal effects on the efficiency of shallow geothermal recovery in long run.

3.2 Effects of phase change temperature

Phase change temperature and latent heat are unique features of mPCM and largely affect heat recovery and storage. The degree of polymerization in the carbon chain of paraffin determines its latent heat magnitude and phase change temperature. While latent heat can be simply treated as additional heat capacity in the material (refer to Fig. 2b for its impact on thermal performance), the phase change temperature governs the liquid or solid state of PCM and thus the exothermic or endothermic processes during ground heat recovery.

The simulations here use the properties of pure paraffin listed in Table 2 for the ground to highlight the melting temperature effect. The paraffin is in a liquid state at the ground initial temperature of 20 °C. Figure 3 presents the time-lapse thermal performance of the energy pile embedded in the PCM ground with different phase change temperature T_{phase}. The results in Fig. 3 are presented in terms of the temperature difference between the ground

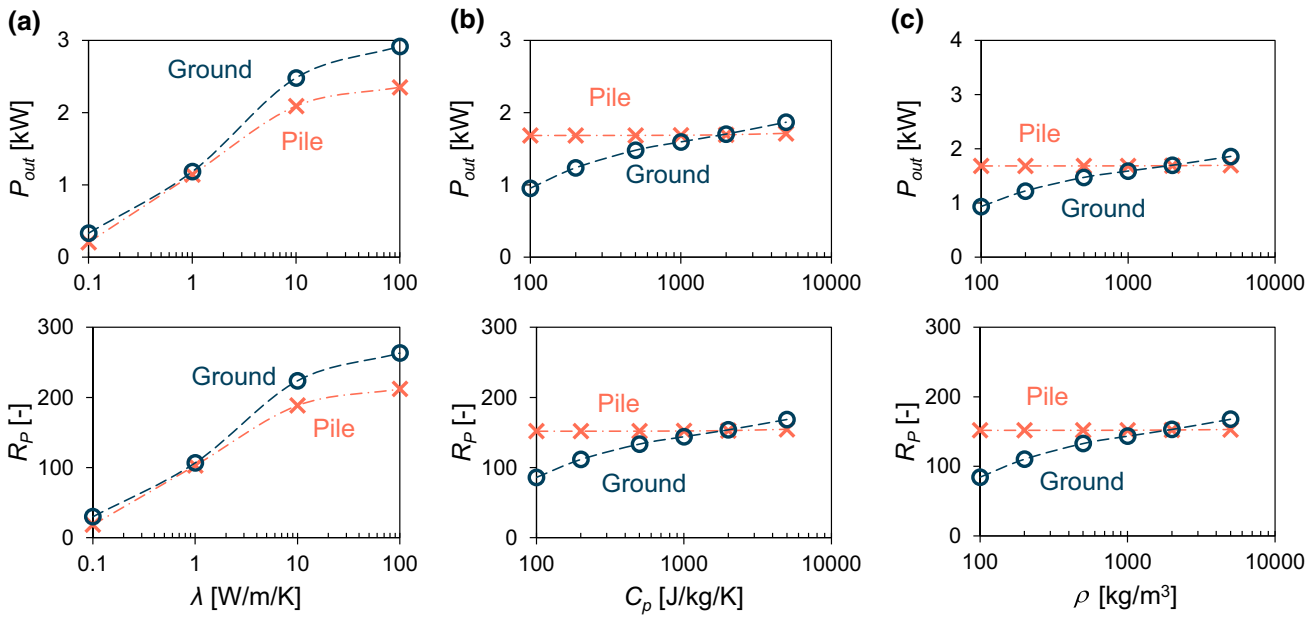

Fig. 2 Effects of thermal properties on thermal performance. **a** Heat conductivity of ground (λ_s) and pile (λ_l). **b** Specific heat capacity of ground (C_s^p) and pile (C_l^p). **c** Density of ground (ρ_s) and pile (ρ_l)

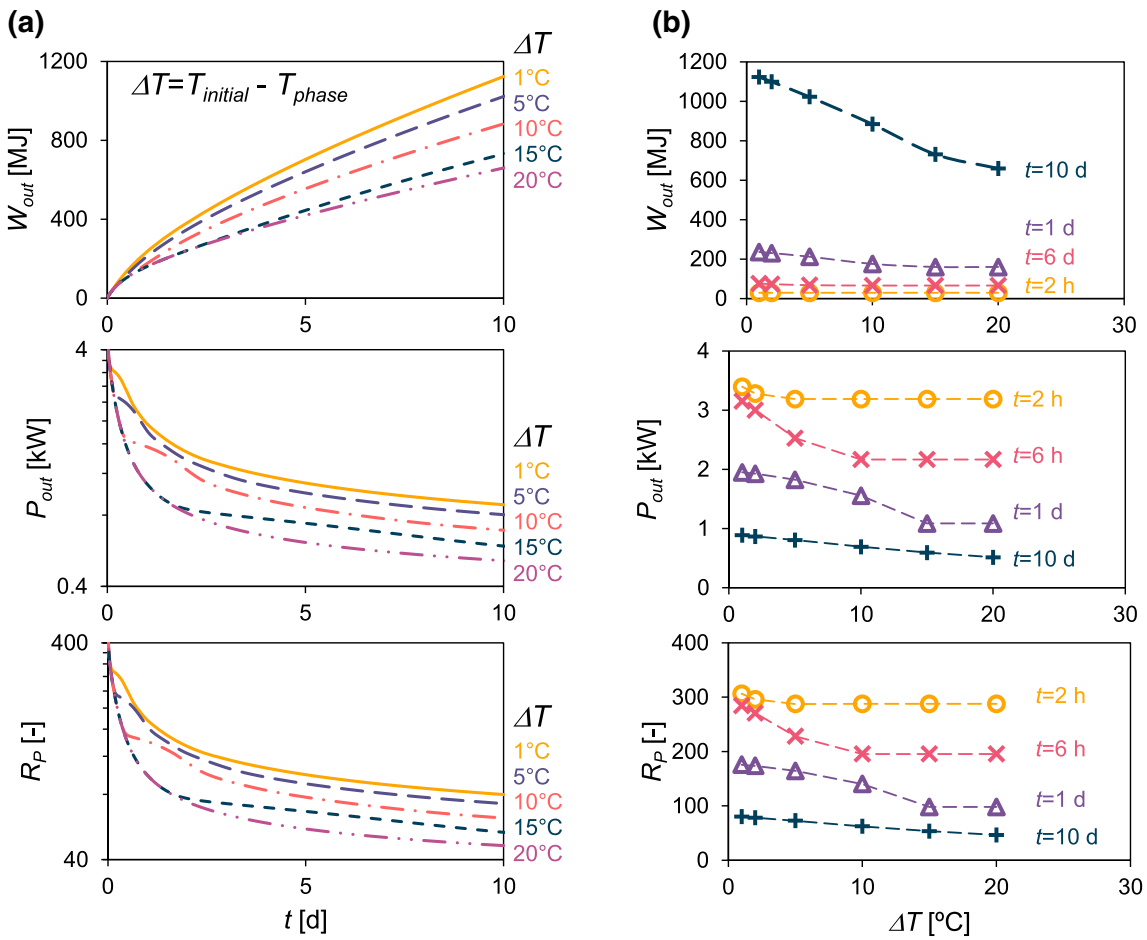

Fig. 3 Effects of the phase change temperature T_{phase} on thermal performance. **a** Time-lapse thermal performance. **b** Thermal performance with different phase change temperatures. Different lines are obtained from various operation time t

initial temperature and the paraffin melting temperature $\Delta T = T_{\text{initial}} - T_{\text{phase}}$. Therefore, ΔT = 1, 5, 10, 15, and 20 °C refers to the phase change temperature of the paraffin which is T_{phase} = 19, 15, 10, 5, and 0 °C, respectively.

The results in Fig. 3a suggest that during the 10-day fluid circulation and heat exchange through the energy pile, the recovered heat energy increases at a decelerated rate. The overall output power and the heat recovery efficiency decrease over time, mainly due to the decreased ground temperature around the pile. In addition, more thermal energy and higher efficiency are achieved at a lower temperature difference between the ground initial temperature and the paraffin melting temperature ΔT. This is because the latent heat is readily approachable in the paraffin with its phase change temperature closest to the ground initial temperature, and thus any small temperature change in the ground due to geothermal recovery can trigger phase change in paraffin, while at larger ΔT, the ground temperature has to be significantly changed during ground heat recovery to reach the paraffin phase change temperature in order to access its latent heat, which is typically not the case for the short-term operation of heat exchangers. One can see in Fig. 3a (P_{out} and R_{P}) that when the phase temperature is reached, a power "surge" is observed. Under the set conditions, this surge occurs earlier for PCM melting temperatures closest to the initial ground temperature.

As shown in Fig. 3b, the output thermal energy, power, and power ratio remain nearly constant in the first 2 h of the heat extraction for all ΔT conditions. After 6 h or 1 day of operation, evident decreases followed by a plateau in the heat energy extraction and the recovery efficiency with increasing ΔT are observed. The plateau starts when the paraffin within the temperature influence zone solidifies and releases latent heat to maintain a constant heat production rate and efficiency. These results again highlight the benefits of using PCM to mitigate the gradual efficiency decrease with the expansion of the temperature influence zone during ground heat extraction.

3.3 Effects of moisture content

The presence of water can significantly increase the thermal conductivity and specific heat capacity of the ground [60]. We here simulate the heat extraction from sands, mPCM, and a sand–mPCM mixture, all in dry or fully water-saturated conditions. The density and thermal properties of the three ground media used in the simulations are listed in Table 2. Note that the porosity of the sand and the mPCM ground are n = 0.4. And the sand–mPCM mixture assumes that the silty size paraffin encapsulates are filling the pores of the sand grain skeleton of n = 0.4, resulting in an effective porosity of n = 0.16 for the mixture. The phase change temperature of the mPCM is set as T_{phase} = 19 °C for all the simulations in this and the following sections.

Figure 4 presents the output thermal energy, the output power, and the output/input power ratio over 10 days of heat exchange with the three ground media in dried and saturated conditions. The results show that the thermal performance, in terms of recovered thermal energy and heat recovery efficiency, is approximately doubled in the sand and the mPCM ground saturated with water than that in the dried condition (Fig. 4a, b). This is mainly because the thermal conductivity of the granular sand or mPCM ground is nearly tripled after saturation, with no significant variation in the thermal diffusivity, which governs the heat front expansion rate. On the other hand, the impact of water saturation on the thermal performance is less pronounced in the sand–mPCM mixture media (Fig. 4c), mainly due to the relatively low porosity and thus less volume fraction of water to enhance the ground thermal properties.

In addition, the results suggest that the sand-mPCM mixture renders the best thermal performance. In the dry condition, the output power P_{out} and power ratio R_{P} from the mixture are 75% greater than that of the pure sand ground and 235% greater than that of the mPCM ground. While in the saturated condition, the P_{out} and R_{P} from the mixture medium are 12% and 104% greater than that of the sand and the mPCM media, respectively. In terms of the total extracted energy W_{out}, the sand-mPCM mixture results in a 65% and 142% higher energy extraction than from the sand and the mPCM media when the ground is in dry condition, and a 14% and 66% higher energy extraction when the sand and the mPCM ground are fully water-saturated. The dry granular mPCM ground gives the lowest geothermal energy production and heat extraction efficiency, mainly due to the relatively low thermal conductivity and thermal diffusivity in the particulate mPCM. Although the thermal properties of the sand and the sand-mPCM mixture ground are comparable, the thermal performance of the energy pile in the mixture media is superior to that in the sand media. This again demonstrates the merits of using phase change materials to enhance shallow geothermal energy recovery with a sustained efficiency.

3.4 60-day operation

Ground heat exchangers are often expected to perform for an extended duration with a periodic on-and-off mode in regions with longer hot or cold seasons. Figure 5 presents the output thermal energy and power ratio from the three dried ground media over 60 days of heat extraction. Note that the extracted thermal energy is in gigawatts in Fig. 5a, while those in Figs. 3 and 4 are in megawatts. Over the entire course of the operation, the fluid is circulated in the

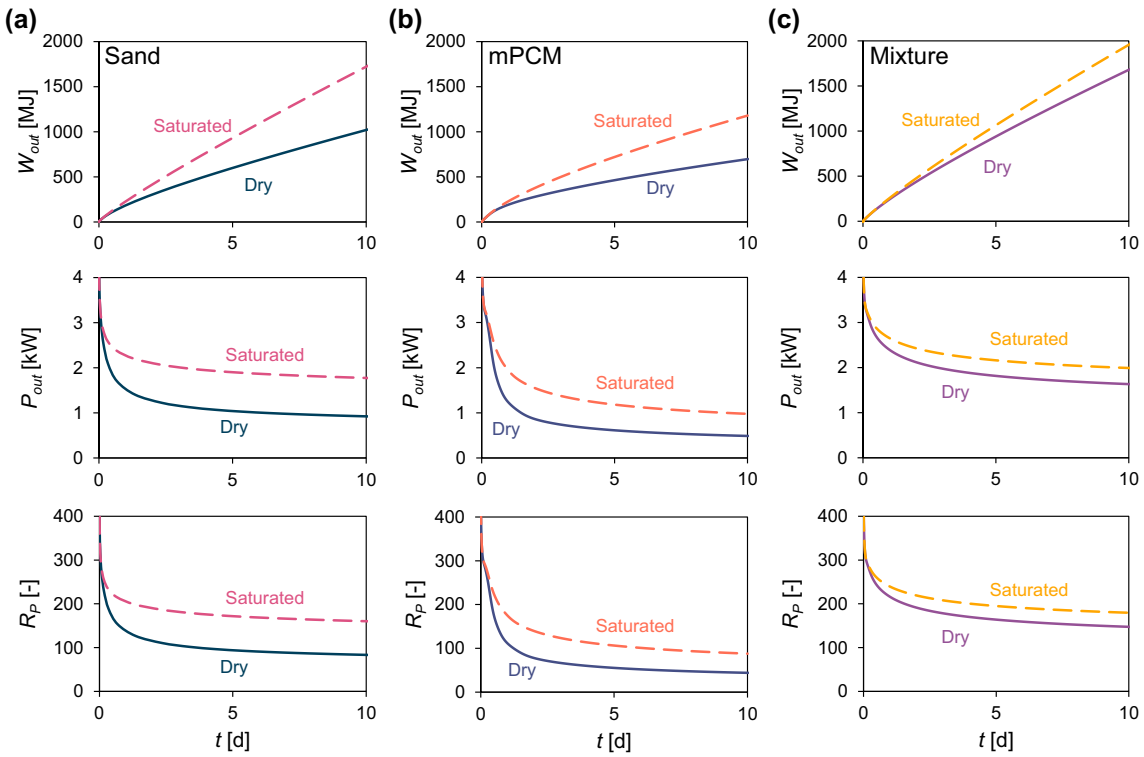

Fig. 4 Effects of the moisture content on thermal performance. Dry and saturated situations are plotted. **a** Pure sand ground domain. **b** Pure mPCM ground domain. **c** Sand–mPCM mixture ground domain

loop continuously for 12 h followed by a 12-h rest each day. For better illustration and comparison among different ground materials, the time-lapse thermal response of each day is condensed into an averaged point in the figures. Note that we fix the domain size to compare the thermal performance difference in each ground medium given the same amount of initial geothermal energy in the reservoir.

The results show that the sand–mPCM mixture gives the best thermal performance than the sand or the mPCM media during the 60 days of heat extraction. At the end of this 60-day operation, the power ratio is reduced by approximately only 1/3 in the sand–mPCM mixture media compared to over 2/3 in the sand or the mPCM media. And the heat exchanging rate (kW) in the mixture is twice that of sand and thrice that of the pure mPCM. The low thermal conductivity and diffusivity of the granular mPCM media hinder the ground heat extraction and result in the lowest output heat power rate and efficiency in the long term as well.

It is worth noting that such simulations are based on a thermal response test setup, where a fast thermal response is expected. The thermal loads considered here are relatively high so that within 60 days of operation, the thermal performance of the simulated system in this study can reach a quasi-steady state, as shown in Fig. 5, while for a commercial geothermal heat exchanger with real-life operation conditions, the sustainability of heat recovery and the long-term unbalanced load will not become significant until after years or even decades of operation given the trend to steady-state conditions observed in the cases studied here [49]. Therefore, the innate thermal response test simulations with high thermal loads for 60 days of operation can be considered as an accelerated long-term thermal response assessment for a commercial ground heat exchanger with real-life operation loads for decades.

3.5 Temperature distribution

Figure 6a illustrates the temperature distribution around the energy pile embedded in the sand versus the sand–mPCM mixture after a 60-day operation. It clearly displays a much lower temperature around the pile and a wider temperature influence zone in the sand media than in the sand–mPCM mixture. Figure 6b contrasts the magnitude of the temperature at a depth of 2 m underneath the ground surface ($z = -2$ m). And Fig. 6c shows the temperature profiles at the same depth across the whole domain. The results indicate that the ground heat exhaustion is constrained within a finite zone in the sand–mPCM mixture, benefited from the PCM in releasing latent heat during fluid circulation and storing ground heat when fluid circulation ceases, while in the sand media, the temperature influence

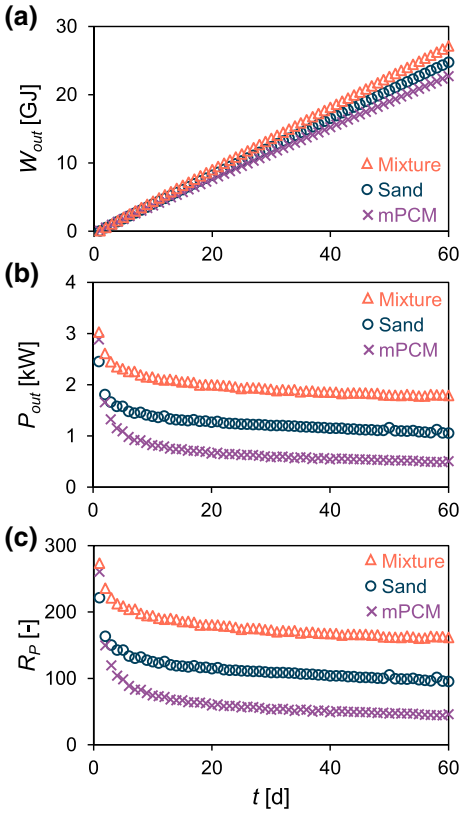

Fig. 5 Effects of long-term operation (cyclic heat extraction for 12 h followed by 12 h of "rest") on the thermal performance of the energy pile embedded in the sand, the mPCM, and the sand–mPCM mixture medium. **a** Output thermal energy W_{out}. **b** Output power P_{out}. **c** Power ratio R_P

zone has reached the domain boundary after 60 days of heat extraction and the boundary temperature has dropped to around 17 °C. According to Fig. 6c, the diameter of the thermally disturbed zone is only half in the sand–mPCM mixture ground compared to that in the pure sand ground. Such a difference in the thermally disturbed zone is expected to be greater in a longer operation time. Therefore, other than enhanced thermal performance and sustained heat recovery efficiency, using mPCM to augment the ground thermal properties can significantly reduce the size of the temperature influence zone. This will minimize the spacing required among heat exchangers to avoid mutual interference, in order to increase the total heat production power per unit volume of the ground. The reduced temperature influence zone can also circumvent potentially legal issues associated with the unintended depletion of neighboring thermal reservoirs or environmental impacts related to groundwater temperature and flow, contaminant dissolution and transport, or biodegradation [11, 19].

3.6 Heat conduction in mPCM enhanced with metal fins

As shown earlier, the mPCM has a large heat capacity (including its latent heat), yet low thermal conductivity and diffusivity (see also Table 2). This will slow down the heat conduction with the far-field ground and make the thermal performance improvement not salient enough. This shortcoming can be mitigated by improving the thermal conductivity of the ground when PCMs are used. Potential methods may include but are not limited to using PCM encapsulated with very high thermally conductive materials like graphene ($\lambda = \sim 4400$ W/m/K) or metal fins offering fast heat conduction paths with the far-field ground.

To illustrate the importance of having a high thermally conductive ground for enhanced geothermal recovery, we here present a case where the energy pile is surrounded by four metal fins (Fig. 7a) that allow fast heat conduction with far field. Note that any materials with high thermal conductivity and diffusivity will serve as a good substitute for the metallic material used here. In this simulation, the energy pile is equipped with 4 steel fins, 1 m wide and 20 mm thick each, embedded in the sand–mPCM mixture ground. The material parameters of the fins are from the COMSOL built-in material library for steel (with a density of 7850 kg/m^3, the specific heat capacity of 475 J/kg/K, and thermal conductivity of 44.5 W/m/K).

Figure 7b presents the time-lapse thermal performance over a 10-day continuous operation of the energy pile embedded in the ground of sand, sand–mPCM mixture, and sand–mPCM–fins medium. The results demonstrate a further improvement in all the geothermal energy production, output power, and heat recovery efficiency by adding four steel fins. This clearly demonstrates that by using metal fins (or high thermally conductive coating) to improve the mPCM ground's thermal conductivity, the objective thermal loads can be achieved within less operating time and the ground heat restoration during "resting" hours can recover at a faster rate. Additional work can be conducted to identify the optimal configuration and design of the fins considering site-specific conditions. Admittedly, metal corrosion, installation, and associated life cycle analyses of using metal fins are not fully considered here and require further investigations.

3.7 Limitations and opportunities

By incorporating latent heat in heat transfer, we show the feasibility of coupled hydrothermal simulation with phase change and the advantages of using mPCMs in approving shallow geothermal recovery. Admittedly, the scenarios

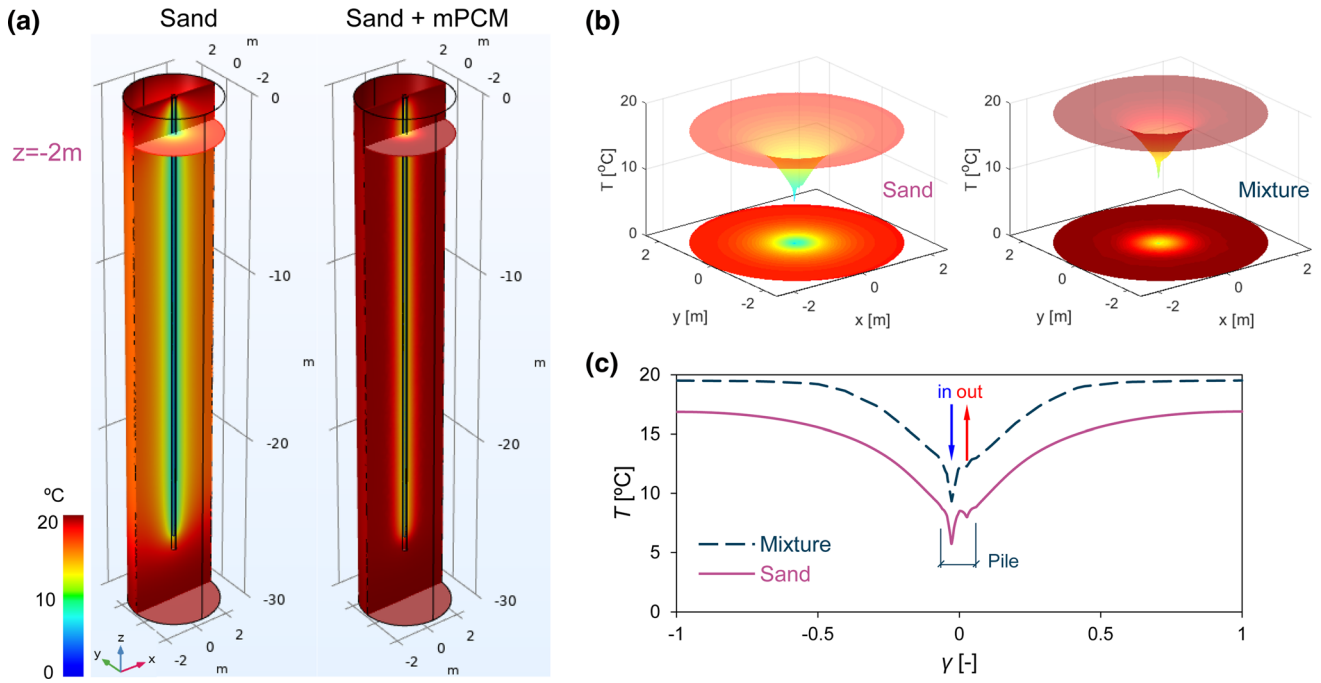

Fig. 6 Temperature distributions after a 60-day operation. **a** Temperature fields in the sand versus the sand–mPCM mixture ground. **b** The temperature contour at a depth of $z = -2$ m. **c** The temperature profiles on the symmetric line of the plane ($y = 0$ m, $z = -2$ m). Here, $\gamma = 2x/d_1$ is a normalized distance in reference to the domain size d_1

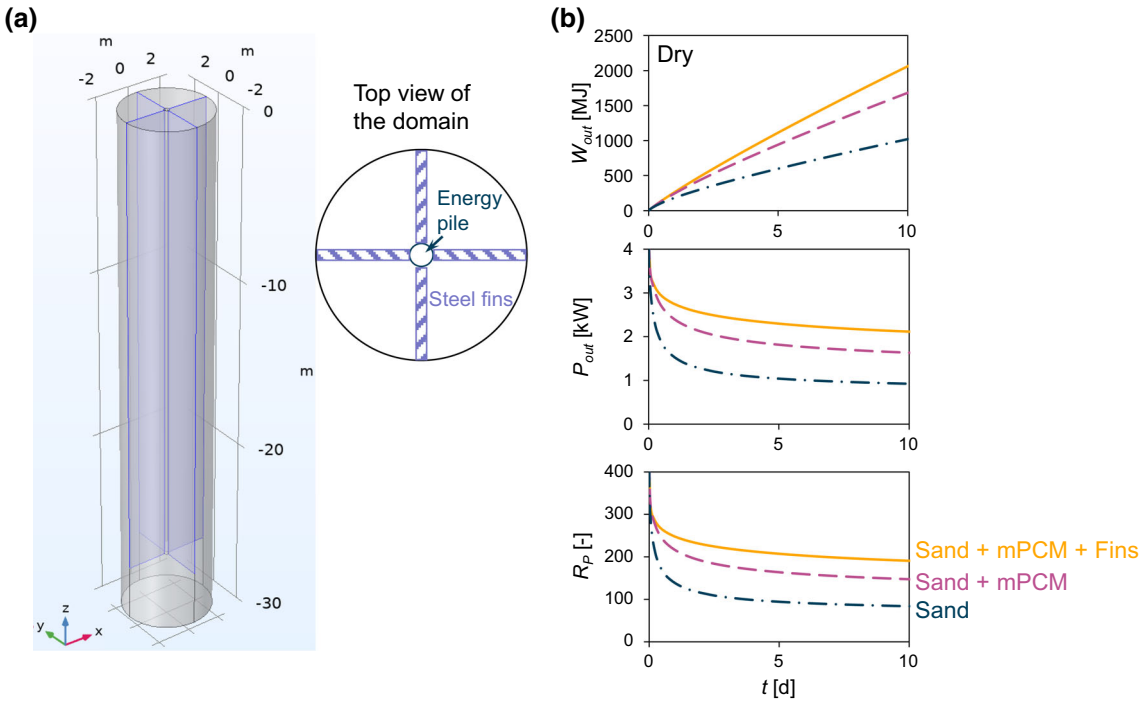

Fig. 7 Thermal performance of an energy pile is enhanced by mPCM and metal fins. **a** An illustration of the energy pile embedded in a sand–mPCM mixture with four steel fins across the domain. **b** The calculated thermal performance over a continuous 10-day heat extraction

considered in this study present certain conceptualized conditions that may oversimplify the actual operational environment of ground heat exchangers. The following considerations are thus imperative for further investigations:

(1) Experimental determination of the thermal, hydraulic, and mechanical properties of soil–mPCM mixtures, considering various environmental conditions including water content and packing.
(2) The longevity of the mPCMs in various types of soils subjected to thermal cycles and groundwater flow, as well as their ensued long-term degradation in the thermal and mechanical properties of soil–mPCM mixtures.
(3) The complexity of the ground stratum, including groundwater conditions, soil layering, surface temperature oscillation, subsurface temperature gradient, and field-scale uniformity of soil–mPCM mixtures, shall be evaluated.
(4) Cost analysis and life cycle analysis of using mPCMs and metal fins, including construction methods, monitoring techniques, corrosion potentials, and maintenance strategies.

While this study presents mostly feasibility assessment, simulated scenarios can be implemented in reality with alternatives, for instance, using anti-freezing solutions instead of water, high thermal conductivity fibers and particles to replace metal fins, and so on. Therefore, bench-scale tests and field pilot tests are in need for the next phase of investigations.

4 Conclusions

In this study, we present numerical investigations that indicate both the short-term and long-term energy pile thermal performance can be significantly improved by modifying the ground with microencapsulated phase change materials and metallic fins. Salient conclusions are drawn as follows.

- The thermal performance of an energy pile is governed by the ground thermal conductivity instead of the specific heat capacity or density. The decrease in thermal performance with time can be mitigated by using mPCM in the ground due to its latent heat. A better performance can be achieved when the phase change temperature closes to the ground temperature. In this case, any small temperature change in the ground due to geothermal recovery can trigger phase change and make the latent heat readily available.
- Both recovered thermal energy and the heat recovery efficiency can be approximately doubled in water-saturated single ground media (sand or mPCM) than that in dried conditions, mainly due to tripled thermal conductivity of the ground media upon water saturation.
- Mixing original ground material (sand) with mPCM can not only improve the thermal performance within short- and long-term operations, but also mitigate the potential environmental issues caused by continuous geothermal recovery. On the one hand, during long-term operation (i.e., 60 days in this study with high thermal loads) of an energy pile, the heat recovery efficiency reduces only 1/3 in the sand–mPCM mixture media compared to over 2/3 in the single sand or granular mPCM media. The overall heat exchange in the sand–mPCM mixture (in kW) is up to two times that of natural sands.
- Using mPCM to augment the ground thermal properties can minimize the spacing required among energy piles to avoid mutual interference, increase the total heat production power per unit volume of the ground, and reduce the temperature influence zone to prevent potential legal or environmental issues such as infringement on neighboring thermal reservoirs and subsurface flow.
- The low thermal conductivity and diffusivity of granular mPCM may slow down the heat conduction with the far-field ground, which makes the thermal performance improvement not salient enough. This shortcoming can be mitigated by implementing a complementary material with high thermal conductivity and diffusivity such as metallic fins around the energy pile.

Acknowledgements This material is based upon work primarily supported by the US National Science Foundation (EEC-1449501 and CMMI-1943722). Any opinions, findings and conclusions, or recommendations expressed in this material are those of the authors and do not necessarily reflect those of the NSF. Data in this manuscript are available upon request. We appreciate the constructive comments from two anonymous reviewers.

References

1. Acuña J, Palm B (2013) Distributed thermal response tests on pipe-in-pipe borehole heat exchangers. Appl Energy 109:312–320
2. Adinolfi M, Loria AFR, Laloui L, Aversa S (2020) Experimental and numerical investigation of the thermo-mechanical behaviour of an energy sheet pile wall. Geomech Energy Environ 25:100208
3. Aditya GR, Mikhaylova O, Narsilio GA, Johnston IW (2020) Comparative costs of ground source heat pump systems against other forms of heating and cooling for different climatic conditions. Sustain Energy Technol Assess 42:100824
4. Aditya GR, Narsilio GA (2020) Environmental assessment of hybrid ground source heat pump systems. Geothermics 87:101868
5. Akrouch GA, Sánchez M, Briaud J-L (2014) Thermo-mechanical behavior of energy piles in high plasticity clays. Acta Geotech 9(3):399–412
6. Akrouch GA, Sánchez M, Briaud J-L (2020) Thermal performance and economic study of an energy piles system under cooling dominated conditions. Renew Energy 147:2736–2747

7. Amatya B, Soga K, Bourne-Webb P, Amis T, Laloui L (2012) Thermo-mechanical behaviour of energy piles. Géotechnique 62(6):503–519
8. Batini N, Loria AFR, Conti P, Testi D, Grassi W, Laloui L (2015) Energy and geotechnical behaviour of energy piles for different design solutions. Appl Therm Eng 86:199–213
9. Bayer P, de Paly M, Beck M (2014) Strategic optimization of borehole heat exchanger field for seasonal geothermal heating and cooling. Appl Energy 136:445–453
10. Beier RA, Acuña J, Mogensen P, Palm B (2013) Borehole resistance and vertical temperature profiles in coaxial borehole heat exchangers. Appl Energy 102:665–675
11. Beyer C, Popp S, Bauer S (2016) Simulation of temperature effects on groundwater flow, contaminant dissolution, transport and biodegradation due to shallow geothermal use. Environ Earth Sci 75(18):1244
12. Bidarmaghz A, Choudhary R, Soga K, Kessler H, Terrington RL, Thorpe S (2019) Influence of geology and hydrogeology on heat rejection from residential basements in urban areas. Tunn Undergr Space Technol 92:103068
13. Bidarmaghz A, Narsilio G (2016) Shallow geothermal energy: emerging convective phenomena in permeable saturated soils. Géotech Lett 6(2):119–123
14. Bidarmaghz A, Narsilio GA (2018) Heat exchange mechanisms in energy tunnel systems. Geomech Energy Environ 16:83–95
15. Bidarmaghz A, Narsilio GA, Johnston IW, Colls S (2016) The importance of surface air temperature fluctuations on long-term performance of vertical ground heat exchangers. Geomech Energy Environ 6:35–44
16. Bottarelli M, Bortoloni M, Su Y, Yousif C, Aydın AA, Georgiev A (2015) Numerical analysis of a novel ground heat exchanger coupled with phase change materials. Appl Therm Eng 88:369–375
17. Brandl H (2006) Energy foundations and other thermo-active ground structures. Géotechnique 56(2):81–122
18. Brigaud F, Vasseur G (1989) Mineralogy, porosity and fluid control on thermal conductivity of sedimentary rocks. Geophys J Int 98(3):525–542
19. Casasso A, Sethi R (2019) Assessment and minimization of potential environmental impacts of ground source heat pump (GSHP) systems. Water 11(8):1573
20. Cecinato F, Loveridge FA (2015) Influences on the thermal efficiency of energy piles. Energy 82:1021–1033
21. COMSOL Multiphysics® v. 5.3a. www.comsol.com. COMSOL AB, S., Sweden Comsol multiphysics pipe flow module user guide (version 5.3a)
22. COMSOL Multiphysics® v. 5.3a. www.comsol.com. COMSOL AB, S., Sweden (2017), COMSOL multiphysics reference manual, pp 674–675
23. Cortes DD, Nasirian A, Dai S (2018) Smart ground-source borehole heat exchanger backfills: a numerical study. In: Paper presented at international symposium on energy geotechnics. Springer, Berlin
24. Cousin B, Loria AFR, Bourget A, Rognon F, Laloui L (2019) Energy performance and economic feasibility of energy segmental linings for subway tunnels. Tunn Undergr Space Technol 91:102997
25. de Paly M, Hecht-Méndez J, Beck M, Blum P, Zell A, Bayer P (2012) Optimization of energy extraction for closed shallow geothermal systems using linear programming. Geothermics 43:57–65
26. Dehdezi PK, Hall MR, Dawson AR (2012) Enhancement of soil thermo-physical properties using microencapsulated phase change materials for ground source heat pump applications. In: Paper presented at applied mechanics and materials. Trans Tech Publ
27. Dunn D (2020) Monthly energy review september 2020 Rep. Energy Information Administration, Office of Energy Statistics, U.S. Department of Energy, Washington, DC
28. Enibe S (2002) Performance of a natural circulation solar air heating system with phase change material energy storage. Renew Energy 27(1):69–86
29. Gao J, Zhang X, Liu J, Li KS, Yang J (2008) Thermal performance and ground temperature of vertical pile-foundation heat exchangers: a case study. Appl Therm Eng 28(17–18):2295–2304
30. Gashti EHN, Malaska M, Kujala K (2015) Analysis of thermo-active pile structures and their performance under groundwater flow conditions. Energy Build 105:1–8
31. Glassley WE (2014) Geothermal energy: renewable energy and the environment. CRC Press, Boca Raton
32. Han C, Yu XB (2016) Sensitivity analysis of a vertical geothermal heat pump system. Appl Energy 170:148–160
33. Han C, Yu XB (2018) An innovative energy pile technology to expand the viability of geothermal bridge deck snow melting for different United States regions: computational assisted feasibility analyses. Renew Energy 123:417–427
34. Jensen-Page L, Narsilio GA, Bidarmaghz A, Johnston IW (2018) Investigation of the effect of seasonal variation in ground temperature on thermal response tests. Renew Energy 125:609–619
35. Kuznik F, David D, Johannes K, Roux J-J (2011) A review on phase change materials integrated in building walls. Renew Sustain Energy Rev 15(1):379–391
36. Liu X, Hughes P, McCabe K, Spitler J, Southard L (2019) GeoVision analysis supporting task force report: thermal applications—geothermal heat pumps *Rep.*, Oak Ridge National Lab.(ORNL), Oak Ridge
37. Loria AFR, Vadrot A, Laloui L (2018) Analysis of the vertical displacement of energy pile groups. Geomech Energy Environ 16:1–14
38. Loveridge F, Powrie W, Nicholson D (2014) Comparison of two different models for pile thermal response test interpretation. Acta Geotech 9(3):367–384
39. Luo J, Zhao H, Gui S, Xiang W, Rohn J, Blum P (2016) Thermo-economic analysis of four different types of ground heat exchangers in energy piles. Appl Therm Eng 108:11–19
40. Makasis N, Narsilio GA, Bidarmaghz A (2018) A machine learning approach to energy pile design. Comput Geotech 97:189–203
41. Makasis N, Narsilio GA, Bidarmaghz A (2018) A robust prediction model approach to energy geo-structure design. Comput Geotech 104:140–151
42. Makasis N, Narsilio GA, Bidarmaghz A, Johnston IW (2018) Ground-source heat pump systems: the effect of variable pipe separation in ground heat exchangers. Comput Geotech 100:97–109
43. Mehrizi AA, Porkhial S, Bezyan B, Lotfizadeh H (2016) Energy pile foundation simulation for different configurations of ground source heat exchanger. Int Commun Heat Mass Transf 70:105–114
44. Narsilio GA, Aye L (2018) Shallow geothermal energy: an emerging technology. In: Low carbon energy supply. Springer, Singapore, pp 387–411
45. Olgun CG, Geyin M, Ozudogru TY (2017) Long-term performance of heat exchanger boreholes at different climatic conditions. In: Geotechnical frontiers 2017, pp 153–164
46. Olgun CG, Ozudogru TY, Abdelaziz SL, Senol A (2015) Long-term performance of heat exchanger piles. Acta Geotech 10(5):553–569
47. Park H, Lee S-R, Yoon S, Choi J-C (2013) Evaluation of thermal response and performance of PHC energy pile: field experiments and numerical simulation. Appl Energy 103:12–24

48. Raymond J, Lamarche L, Malo M (2015) Field demonstration of a first thermal response test with a low power source. Appl Energy 147:30–39
49. Rybach L, Mégel T, Eugster W (2000) At what time scale are geothermal resources renewable. In: Paper presented at proceedings world geothermal congress 2000
50. Sani AK, Singh RM, Amis T, Cavarretta I (2019) A review on the performance of geothermal energy pile foundation, its design process and applications. Renew Sustain Energy Rev 106:54–78
51. Self SJ, Reddy BV, Rosen MA (2013) Geothermal heat pump systems: status review and comparison with other heating options. Appl Energy 101:341–348
52. Sharma A, Tyagi VV, Chen C, Buddhi D (2009) Review on thermal energy storage with phase change materials and applications. Renew Sustain Energy Rev 13(2):318–345
53. Tsagarakis KP (2020) Shallow geothermal energy under the microscope: social, economic, and institutional aspects. Renew Energy 147:2801–2808
54. Ukrainczyk N, Kurajica S, Šipušić J (2010) Thermophysical comparison of five commercial paraffin waxes as latent heat storage materials. Chem Biochem Eng Q 24(2):129–137
55. Wang JL, Zhao JD, Liu N (2014) Numerical simulation of borehole heat transfer with phase change material as grout. In: Paper presented at applied mechanics and materials. Trans Tech Publ
56. Waples DW, Waples JS (2004) A review and evaluation of specific heat capacities of rocks, minerals, and subsurface fluids. Part 1: minerals and nonporous rocks. Nat Resour Res 13(2):97–122
57. Waqas A, Din ZU (2013) Phase change material (PCM) storage for free cooling of buildings—a review. Renew Sustain Energy Rev 18:607–625
58. Weast RC, Astle MJ (1983) CRC handbook of chemistry and physics: 1983–1984. CRC Press, Boca Raton
59. You S, Cheng X, Guo H, Yao Z (2016) Experimental study on structural response of CFG energy piles. Appl Therm Eng 96:640–651
60. Yun T, Santamarina J (2008) Fundamental study of thermal conduction in dry soils. Granul Matter 10(3):197–207. https://doi.org/10.1007/s10035-007-0051-5
61. Zarrella A, De Carli M, Galgaro A (2013) Thermal performance of two types of energy foundation pile: helical pipe and triple U-tube. Appl Therm Eng 61(2):301–310
62. Zhang Y, Soga K, Choudhary R (2014) Shallow geothermal energy application with GSHPs at city scale: study on the City of Westminster. Géotech Lett 4(2):125–131